Turk J Phys
32 (2008) , 227 – 234.

Optical and Structural Properties of the GaS_xSe_{1-x}, GaSe, $TlGaSe_2$ and $TlInS_2$ Semiconductors

Aydın ULUBEY KULIBEKOV
Department of Physics, Faculty Art and Science, Trakya University,
22030 Edirne-TURKEY
e-mail: aydinanar@yahoo.co.uk

Received 06.11.2007

Abstract

In the present work, crystal structure and optical properties of the layered chalcogenides GaS_xSe_{1-x}, GaSe, $TlGaSe_2$ and $TlInS_2$ were investigated in the visible (VIS) and infrared (IR) range of spectra. Partial content of the elements were performed and the space group were determined by help of X-ray diffraction experiments. Making use of the experimental results, we have constructed a scheme of band motion for the transition from GaSe to GaS. It has been established that that the infrared active optical modes show typical two-mode behaviour.

DOI: 10.1007/s10762-005-0294-3, 10.1063/1.2128694

Key Words: Chalcogenides, layered semiconductors, optical properties, vibrational modes, multiphonon absorption, crystalline and band structure, correlation analysis.

1. Introduction

GaSe-GaS solid solutions crystallize in easily cleavable layers, consisting from 4 atoms in the sequence Ga-Se(S)-Se(S)-Ga. Within layers the atoms are connected by strong ionic covalent bonding, whereas forces between layers are of van der Waals type. If one examines an isolated layer of GaSe(S), one may consider that it is produced by stacking of the two hexagonal planes, analogous to those of graphite, where in each plane three Ga atoms surround each Se, and vice-versa three Se atoms surround each Ga atom. These two sub-layers are bound together by Ga-Ga bridges, which deform the two hexagonal lattices (see Figures 1 and 2). The parameters of unit cell for ε-GaSe (organized in the D^1_{3h} space group, with two layers per unit cell) are: $a = 3.749$ Å, $c = 16.05$ Å, $c/a = 4.25$ [1, 2]. GaS has similar structure and parameters. In the stacking direction (i.e. along the crystallographic z-axis) the layers can be arranged in different ways, which leads to the existence of different polytypes [1].

Though there are several works devoted to the physical properties of $GaS_{1-x}Se_x$ crystals, there is still need to investigate a change of the optical properties. This study will help to clarify the mechanism for the intercalation of solid solutions.

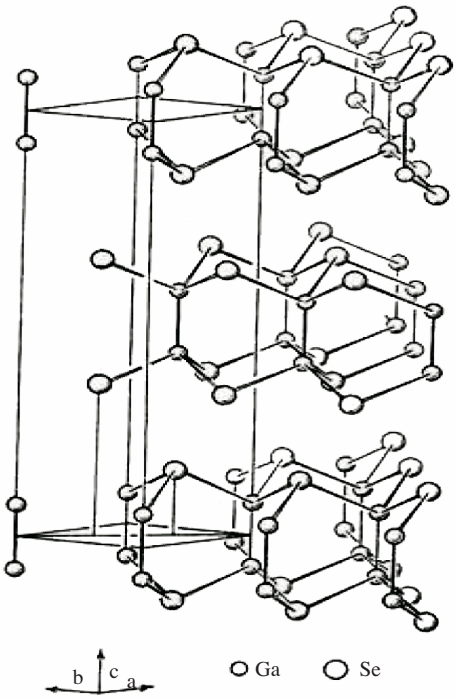

Figure 1. The crystal structure of hexagonal ε-GaSe.

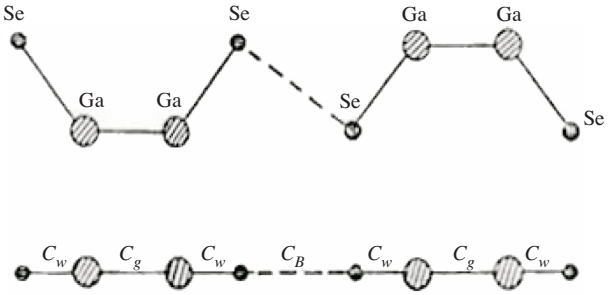

Figure 2. The stacking of layers in GaSe.

High anisotropy of the bonds between the atoms makes it easy to obtain thin films of the layered crystals. The ternary $TlGaSe_2$ and $TlInS_2$ crystals have a number of interesting properties [3–6]. They have a monoclinic structure with the a- and b-axis in the plane of the layer and with the optical c-axis perpendicular to layers. A main structural unit is the two-dimensional periodic layer, consisting from the group of tetrahedra. Each tetrahedra group consists of 4 elemental tetrahedra of $Ga(In)Se_4(S_4)$ (see Figure 3).

2. Experiment

The materials were synthesized by the horizontal method in evacuated quartz ampoules. At the beginning the ampoule, with the stoichiometric amounts of materials, was loaded into a horizontal furnace. The end of the furnace has a temperature near the melting temperature of the respective material. It is at this temperature the exothermic reaction begins in the ampoule.

As reaction finished, the ampoule was removed to a deeper part of the furnace. It took about 6 hours to complete this process. With the ampoule remaining inside, the furnace was vertically reoriented; the vertical position was maintained for a further 6 hours, with the temperature at the material's melting point. Via

a special device, connected by quartz rod, the ampoule was shook for the 6 hours, to obtain homogenous material. After homogenization, the crystals were grown by the Bridgman method.

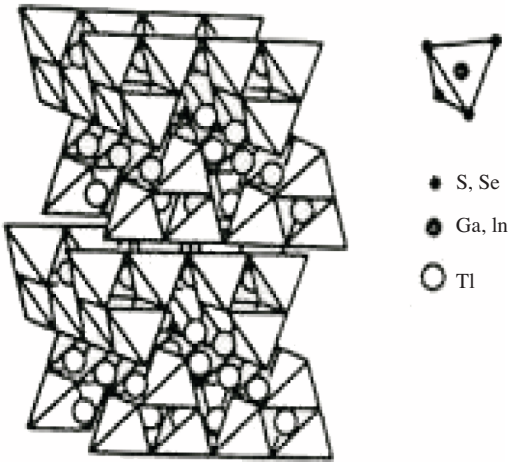

Figure 3. Stacking of the anionic layers and positions of Tl^+ ions between them.

The quality of the crystallization was examined using a X- ray fluorescence spectrometer. Analysis were made from samples taken from different sections of the ampoule: top, middle and end. Analysis showed that diffraction lines corresponding to only the synthesized materials were present.

Non-doped $GaS_xSe_{1-x}(x = 0, 0.2, 0.4, 0.47, 0.6, 0.8, 1.0)$ crystals were grown by Bridgman method in evacuated quartz tubes (10^{-5} Torr). Thermoelectric testing showed that all samples were p-type. The crystals were characterized by a Shimadzu XDR-600 X-ray diffractometer (CuKα, $\lambda = 1.5405$ Å) and the X-ray fluorescence (XRF) measurements.

Visible (VIS) and infrared (IR) transmission spectra were characterised at room temperature by using a Shimadzu 1601 spectrometer (0.4–0.8 μm) and a Perkin Elmer Spectrum BX II FTIR spectrometer (2.5–26 μm). Depending on the signal to noise ratio, we choose a certain scan speed and the width of the slit with the aim to obtain high resolution (±2–3 cm^{-1}).The measurements were performed using two- and one-beam method. The accuracy of transmission measurements was not worse than ±2%. The thicknesses of the samples varied in the range from 10 μm to 2 mm. All measurements were performed at room temperature.

3. Results and Discussion

The X-ray diffraction and fluorescence peaks for GaSe indicate for ε-modification with the lattice parameters $a = b = 3.749$ Å, $c = 15.907$ Å, c / $a = 4.2430$. For $TlGaSe_2$ $a = 15.632$ Å, $b = 10.773$ Å, $c = 10.744$ Å, a / $c = 1.4502$.

The fractional species content of GaSe, $TlGaSe_2$, $TlInS_2$ samples used in the present study are listed in Table 1. $TlGaSe_2$ and $TlInS_2$ may be considered as monoclinic space group (C^s_{2h}), while GaSe and GaS are considered hexagonal (D^1_{3h}).

Figures 4–6 represent the transmission spectra of GaSe in the range of 0.4–0.8 μm at room temperature (300 K). Direct band gap was determined from analysis. For $TlGaSe_2$: 602 nm; for $TlInS_2$: 536 nm; for GaSe: 619 nm.

Figures 7–9 show the infrared transmission spectra of these crystals in the spectral range of 2.2–26 μm, at room temperature. Comparisons of our results with those in the literature are shown in Tables 1–3.

Table 1. Transmission data, both present experimental and that reported in literature, for GaSe.

Experiment		Literature [3, 4, 5, 6, 7]
Wavenumber, in cm^{-1}	Wavelength, in μm	Wavenumber, in cm^{-1}
477.93	20.92	482 (IR-absorption)
477.93: 2=239	41.84	236 (A_2, IR reflection, ω_{TO}, E $\perp$ c)
510.74	19.58	512 (IR absorption, E $\perp$ c)
510.74: 2=255	39.22	254.7 (IR transmission, ω_{LO}, E $\perp$ c)
538.35	18.58	540 (IR absorption, E $\perp$ c)
618.93	16.16	618 (IR absorption)
618.93: 2=309	32.36	308 (Raman, A_1')
618.93: 3=206	48.54	211 (IR transmission, ω_{TO}, E $\perp$c)
667.25: 3=222	45.05	230.7 (IR transmission, ω_{TO}, E $\perp$c)
1079.9: 2=540	18.52	540 (IR absorption, E $\perp$c)

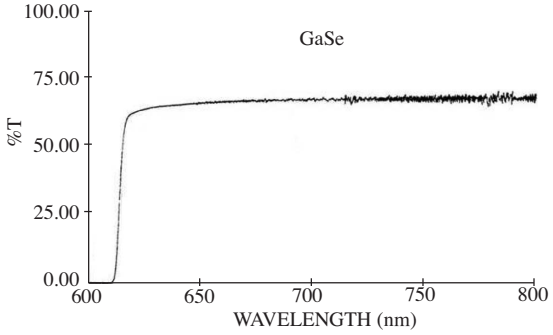

Figure 4. Transmission spectrum for GaSe monocrystalline in the visible region.

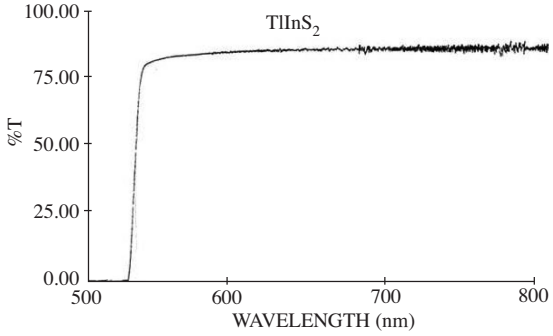

Figire 5. Transmission spectrum for $TlInS_2$ monocrystalline in the visible region.

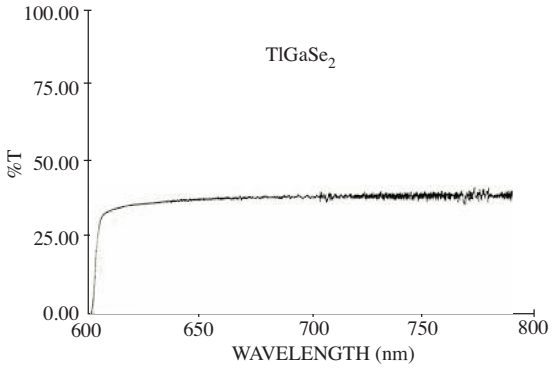

Figure 6. Transmission spectrum for $TlGaSe_2$ monocrystalline in the visible region.

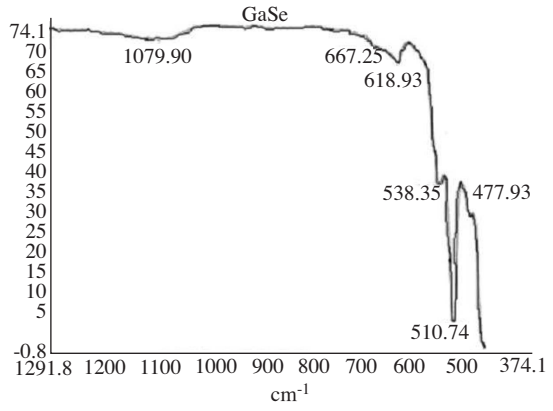

Figure 7. Transmission spectrum for GaSe monocrystalline in the infrared region.

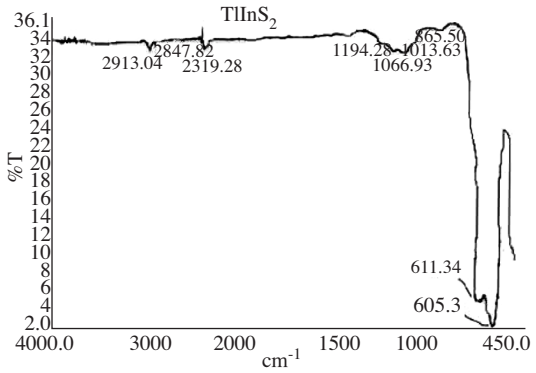

Figure 8. Transmission spectrum for $TlInS_2$ monocrystalline in the infrared region.

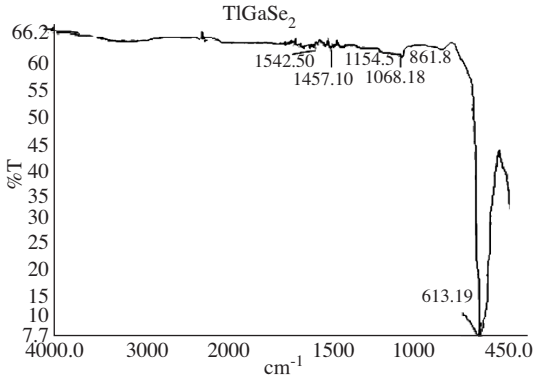

Figure 9. Transmission spectrum for $TlGaSe_2$ monocrystalline in the infrared region.

Table 2. Transmission data, both present experimental and that reported in literature, for $TlInS_2$.

Experiment		Literature [3, 4, 5, 6, 7]
Wavenumber, in cm^{-1}	Wavelength, in μm	Wavenumber, in cm^{-1}
605.30: 2=303	33.00	295 (IR-reflection, $\omega_{TO,}$ E $\perp$c) 302 (Raman)
872.70: 3=291	34.36	295 (IR-reflection, $\omega_{TO,}$ E $\perp$c) 292 (Raman)
622.34: 2=306	32.68	302 (Raman)
865.50: 3=289	34.66	295 (IR-transmission, $\omega_{LO,}$ E $\perp$ c)
1013.63: 3=338	29.60	348 (IR-absorption, E $\perp$ c)

Table 3. Transmission data, both present experimental and that reported in literature, for $TlGaSe_2$.

Experiment		Literature [3, 4, 5, 6, 7]
Wavenumber, in cm^{-1}	Wavelength, in μm	Wavenumber, in cm^{-1}
677.60: 3=226	44.28	228 (IR-reflection, $\omega_{TO,}$ E $\perp$c) 230 (Raman)
487.05: 2=244	40.98	238 (IR-reflection, $\omega_{TO,}$ E $\perp$c)
487.05: 3=162	61.73	163 (Raman)
603.19: 3=201	49.75	198 (Raman)

Tables 1–3 show that TO-phonons for these crystals are present in E$\perp$c geometry, where E is the electric field vector of the incident light, and c refers to the optical axis of the crystal. One, two and three phonon absorption are seen in the spectra shown in Tables 1–3. According to the symmetry selection rules A''_2 type phonons are IR active in E $\perp$c, whereas A'_1 phonons are active in Raman scattering. Analysis showed that a number of phonons observed in our experiments are less than that predicted by the group theoretical analysis for C^2_{2h} space group. This fact says in a favour that $TlGaSe_2$ and $TlInS_2$ crystals do not belong to C^2_{2h} space group.

Comparison of our results with those predicted by the theory of symmetry shows that the best agreement is observed if we suppose that the elementary unit cell of studied crystals consists of two layers with the symmetry of layer D^{18}_{4h} (TlSe space group) and the crystals have C^6_{2h} space group. Correlation analysis gives the following phonons in k=0:

$$\Gamma_{vib}(C^6_{2h}) = 10A_g + 10A_u + 14B_g + 14B_u,$$

from which $A_g + A_u$ and $2B_g + 2B_u$ are rigid layer modes and $A_u + 2B_g$ are acoustic vibrations. One may see that the number of phonons observed in the experiment and those predicted by the theory of symmetry are in accordance with C^6_{2h} space group of studied $TlGaSe_2$ and $TlInS_2$ crystals.

For GaSe crystal the irreducible representations at $k = 0$ for D^1_{3h} space group are:

$$\Gamma_{vib}(D^1_{3h}) = 4A'_1 + 4A''_2 + 4E' + 4E''.$$

In this case there are 11 non-degenerate Raman ($4E''$,$4A'_1$,$3E'$) and 6 IR active phonons ($3A''_2$, 3E/). Comparison with experiments gives A''_2 symmetry for 239 cm^{-1} phonon band and A_1/-type for band at 309 cm^{-1}. In our consideration we admit simultaneous activity of IR and Raman active phonons.

Symmetry of phonons, the direction of displacement of atoms and the symmetry selection rules for ε-GaSe are presented in Figure 10. Optical measurements of the absorption edge of $GaS_{1-x}Se_x$ crystals are shown in Figure 11.

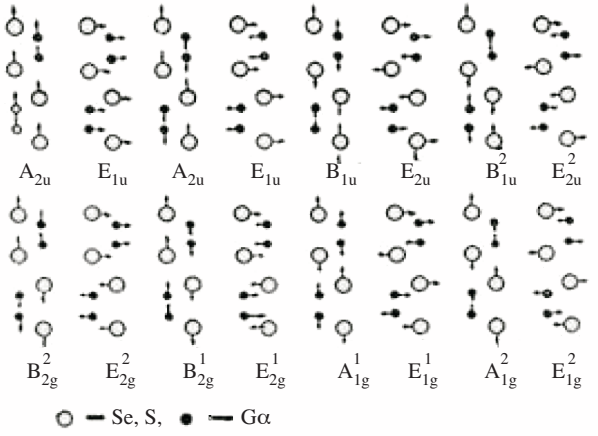

Figure 10. Atomic displacement vectors for interlayer and intralayer Raman-active optical modes of ε-GaSe.

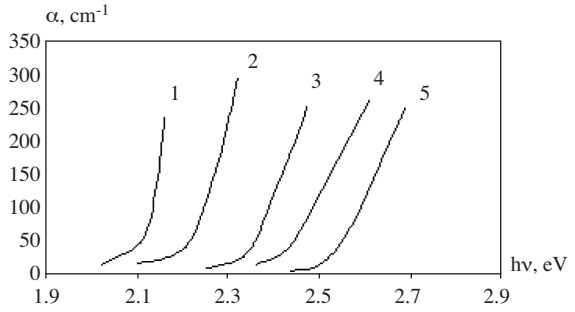

Figure 11. Edge absorption spectra of GaS-GaSe mixed crystals. 1.GaSe 2.$GaS_{0.4}Se_{0.6}$ 3.$GaS_{0.47}Se_{0.53}$ 4. $GaS_{0.6}Se_{0.4}$ 5.GaS.

The absorption coefficients, were obtained from the transmission data, using the relation T=(1-R)^2 exp(-αd), where T is the transmissivity, R is the reflectivity, d is the sample thickness and α is the absorption coefficient. Analysis of these curves shows that the absorption spectra can be described by the formula $\alpha^k = A(h\gamma\text{-}E_g)$, where $k = 2$ for direct allowed transitions and $k = 0.5$ for indirect allowed transitions (low energy part of the spectra).

The obtained experimental data verify that the band gap values exhibit a different dependence upon composition. Since the account of three-dimensionality influences the valence band positions rather weakly [9], we use the theoretical calculations [10] performed in the tight-binding approach. It turned out that the $\sqrt{}$ point shifts by 900 and 800 meV for direct and indirect transitions when we replace Se by S. Making use of the experimental results outlined in Figure 11, we have constructed in Figure 12 the scheme of band motion for the transition from GaSe to GaS.

By our experimental results the bottom of the conduction band at the $_3$ point and the bottom of the conduction band at the K_1 point are shifted by 410 and 405 meV, respectively (see Figure 11).

The dependence of the energetic position of edge absorption upon x is presented in Figure 13. The dependence is linear over the whole range $0 \leq x \leq 1$. Comparison of experimental and theoretical calculations verifies that the band gap values exhibit a different dependence upon composition. We can consider such a transition as effective deformation of GaSe. The characteristic energy shifts can directly be related to atomic spectral properties of sulphur and selenium.

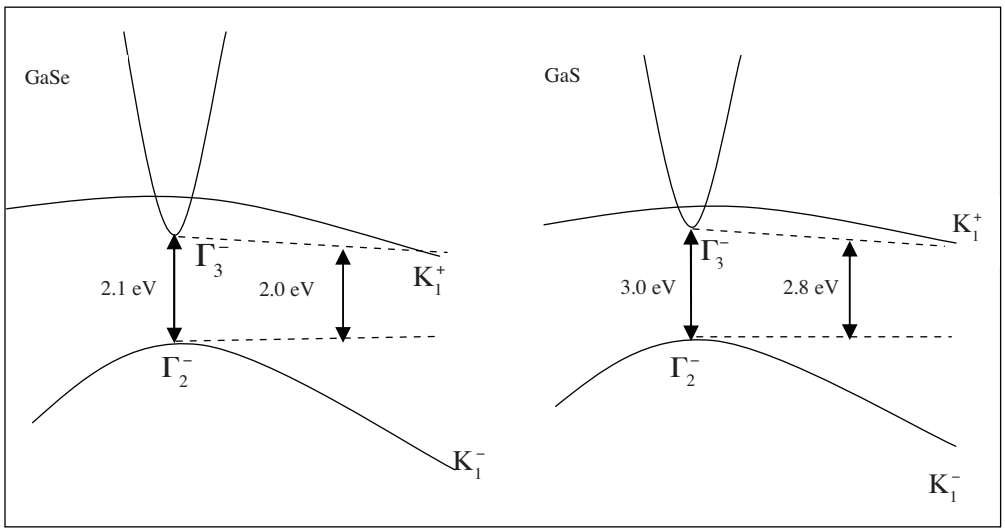

Figure 12. Band shift scheme.

The lattice vibrational properties of $GaS_{1-x}Se_x$ mixed crystals have been studied by Raman and absorption measurements [11]. It has been established that that the infrared active optical modes show typical two-mode behaviour. The composition dependence of the infrared active optical mode frequencies can be described by the modified random element iso-displacement (MREI) [12]. The occurrence of both the GaS-like and GaSe-like modes in the mixed crystals and the linear dependence of their oscillator strengths on composition are typical for two mode behaviour [12]. As can be seen from Figure 14, the composition dependence of the force constants is influenced by the composition dependence of the lattice parameters [13]. The strength of each phonon mode of the mixed crystal is proportional to the mole fraction of the component it represents. The account for the behaviour of a mixed crystal system has considered in [14]. Model [14] does predict two optical modes and shows a fair over-all agreement with experiment. The theory [12] to predict whether a crystal $AB_{1-x}C_x$ will show one-mode or two-mode behaviour and also the dependence of the optic phonon frequencies on the mode fraction x.

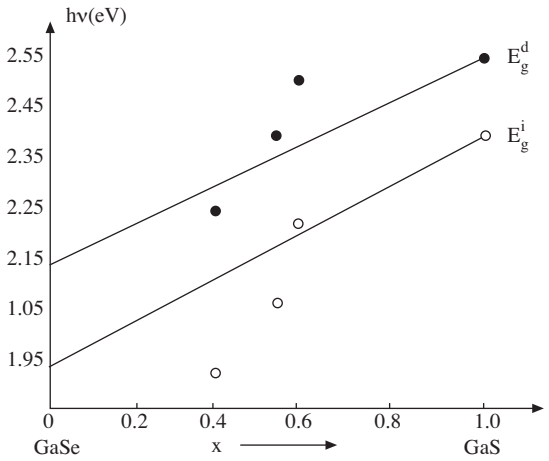

Figure 13. The dependence of the energetic position of the edge absorption upon x.

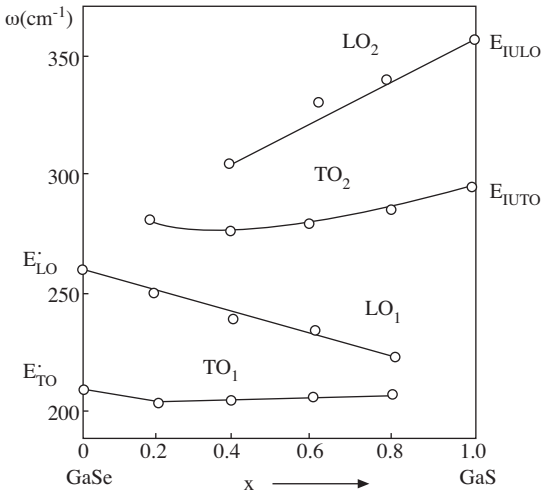

Figure 14. Concentration dependence of longitudinal (LO) and transverse (TO) optical model frequencies. Points indicate the position of the experimentally observed lines;full lines are calculated according to the (MREI)[12] model.

The dependence of the frequencies phonons on the compositions of solid solutions are depicted on Figure 14.

As a whole, these dependences are in agreement with the data presented in [11]. The low frequency region of the spectrum showed an interlayer shear mode at all the concentration of solid solutions. Local vibration of S in GaSe and the gap mode frequency of Se in GaS equal to 280 and 210 cm^{-1}, respectively.

4. Conclusion

Multiphonon absorption is seen in infrared spectra of GaSe, GaS, $TlGaSe_2$ and $TlInS_2$ semiconductors. Correlation analysis is in agreement with experiment.

From the functional dependence obtained for the absorption coefficients on photon energies it may be inferred that the GaS-GaSe mixed crystals show also indirect transmission across the energy gap in agreement with band calculations. From vibrational spectra of this crystals two-mode behaviour and nonlinear change of the force constants with composition is found.

Acknowledgements

This material is based upon work supported by the Turkish Scientific and Technical Research council, TUBİTAK under Project No. TBAG-2220(102T113).

References

[1] K. Allakhverdiev, S. Hana, A. Kulibekov(Ulubey), S. Özbek, E. Gunay, D. Huseinova, *International Journal of Infrared and Millimeter Waves*, **26**, (2005), 1741.

[2] Z. Samedov, O. Baykan, A. Gulubayov, *International Journal of Infrared and Millimeter Waves*, **25**, (2004), 735.

[3] K. Allakhverdiev, N. Fermelius, F. Gashimzade, J. Goldstein, E. Salaev, Z. Salaeva, *J. Applied Phys*, **93**, (2003), 3336.

[4] E. Finkman, A. Rizzo, *Solid State Commun.*, **15**, (1974), 1841.

[5] J. Irwin, R. Hoff, B. Clayman, R. Bramley, *Sol. State Commun.*, **13**, (1973), 1531.

[6] T. Wieting, J. Verole, *Phys. Rev.*, **B5**, (1972), 1473.

[7] P. Leung, *J. Phys. Chem. Sol.*, **27**, (1966), 849.

[8] K. Allakhverdiev, Ph.D. Thesis, Dept. of Physical and Mathematical Sciences, Institute of Physics, Baku, Azerbaijan, 1980.

[9] M. Schluter, *Nuovo Cimento*, B**13**, (1973), 313.

[10] H. Kamimura, K. Nakao, *J. Phys. Soc. Japan*, **24**, (1968), 1313.

[11] K. Allakhverdiev, M. Tagyev, *Phys. Stat Sol.*, **(a)39**, (1977), K11.

[12] I. Chang, S. Mitra, *Adv. Phys.*, **20**, (1971), 359.

[13] C. Whitehouse, A. Balchin, *Jour. Mater. Sci.*, **13**, (1978), 2394.

[14] D. Langer, *Phys. Rev.*, **152**, (1966), 778.